Spherical Cavity Expansion in Material with Densification

Introduction

Fused silica (SiO_2) exhibits some unique features when it is ground or polished. It also densifies permanently under large compressive stresses at room temperature;[1–3] up to 15% permanent densification has been observed.[2,3] The experimental data for densification from different works, however, are obviously inconsistent,[4] which may result from different levels of shear stresses present in the experiments. The molecular dynamics simulation by Tse *et al.*[5] proved this suggestion by showing that the densification is caused by extensive bending of atomic bonds, even under pure hydrostatic pressure. Based on these observations, a new constitutive law was suggested by Lambropoulos *et al.*[6] for this kind of material.[7]

To understand the material behavior under compression, the cavity expansion problem is solved analytically. Both associated and non-associated flow theories have been studied. A densification parameter has been introduced in the proposed material model. The material is assumed to be perfectly plastic; however, the introduction of densification produces an effect similar to hardening.

Constitutive Model

The traditional shear flow theory cannot describe the plastic behavior of fused silica because the permanent densification is so large that its effects cannot be neglected. Experiments and observations on fused silica have suggested that the shear will facilitate the densification.[4,5,7] Lambropoulos *et al.*[6] suggested a new material model to describe this kind of material. The yield surface is defined by the effective stress

$$\sigma_e = -\alpha\sigma_m + (1-\alpha)\tau_e, \tag{1}$$

where

$$\sigma_m = \frac{1}{3}\sigma_{kk} = \frac{1}{3}\left(\sigma_{11}+\sigma_{22}+\sigma_{33}\right),$$

$$\tau_e = \sqrt{\frac{1}{2}s_{ij}s_{ij}}\,, \quad s_{ij} = \sigma_{ij} - \sigma_m\delta_{ij},$$

and α is the densification parameter, which ranges from 0 to 1. Here the summation convention is used. δ_{ij} is the Kronecker delta. For pure hydrostatic compression, where $\sigma_{11} = \sigma_{22} = \sigma_{33} = -p$, the mean hydrostatic stress $\sigma_m = -p$ and effective shear $\tau_e = 0$. For pure shear, $\sigma_m = 0$ and $\tau_e = |\tau|$. For uniaxial tension, $\sigma_m = \sigma/3$ and $\tau_e = \sigma/\sqrt{3}$. Notice that τ_e is always positive.

The material yields when $\sigma_e > Y$. The normal of yield surface can be expressed as

$$\mu_{ij} = \frac{\partial f}{\partial \sigma_{ij}} = -\frac{\alpha}{3}\delta_{ij} + \frac{(1-\alpha)}{2}\frac{s_{ij}}{\tau_e}. \tag{2}$$

When the inner product $\mu_{ij}d\sigma_{ij} > 0$, the small change of stress $d\sigma_{ij}$ causes further deformation loading. When $\mu_{ij}d\sigma_{ij} < 0$, it is unloading. Permanent strains ε_{ij}^p evolve as

$$d\varepsilon_{ij}^p = \begin{cases} 0, & \text{if } \mu_{ij}d\sigma_{ij} \le 0 \\ \neq 0, & \text{if } \mu_{ij}d\sigma_{ij} > 0 \end{cases}. \tag{3}$$

With continued loading, we assume that the permanent strains are not affected by the rate of loading; thus, the flow rule gives

$$d\varepsilon_{ij}^p = d\lambda\frac{\partial g}{\partial \sigma_{ij}}, \quad g\left(\sigma_{ij}\right) = -\alpha'\sigma_m + (1-\alpha')\tau_e, \tag{4}$$

where $g(\sigma_{ij})$ is the flow potential. Generally the material constant α' in Eq. (4) is different from α in Eq. (1), which is called the non-associated flow theory. For special case $\alpha = \alpha'$, called the associated flow theory, the permanent strain increment is normal to the yield surface in stress space.

By using the principle of plastic work equivalence $\sigma_{ij}d\varepsilon_{ij}^p = c\sigma_e d\bar{\varepsilon}^p$, where c is a numerical factor, the plastic strain increment can be solved as

$$d\varepsilon_{ij}^{p} = \frac{d\bar{\varepsilon}^{p}}{C}\left(-\frac{\alpha'}{3}\delta_{ij} + \frac{1-\alpha'}{2}\frac{s_{ij}}{\tau_e}\right), \tag{5}$$

where

$$C = \sqrt{\frac{2}{9}\alpha'^{2} + \frac{1}{3}(1-\alpha')^{2}}\,.$$

For a standard elastic theory (Hooke's law), the elastic strain increment is

$$d\varepsilon_{ij}^{e} = \frac{1}{2G}ds_{ij} + \frac{(1-2\nu)}{E}\delta_{ij}d\sigma_{m}\,, \tag{6}$$

where G is shear modulus, defined as $G = E/2(1+\nu)$. Then the total strain increment is given by

$$d\varepsilon_{ij} = d\varepsilon_{ij}^{e} + d\varepsilon_{ij}^{p}\,. \tag{7}$$

The incremental stress–strain relation, written in tensor format, is

$$d\sigma_{ij} = D_{ijkl}\,d\varepsilon_{kl}\,, \tag{8}$$

where the fourth-order tensor D_{ijkl} is the material's incremental constitutive law matrix.

Cavity Expansion

A spherical cavity embedded in an infinite medium with an initial radius a_0 is subjected to inner pressure P. With the increase of P, the cavity wall expands. When the pressure is larger than the initial yield pressure P_c, a plastic zone forms outside the cavity wall. Due to the symmetry, a spherical polar Lagrangian system (r, θ, φ) at the center of the cavity has been used. The material deforms only along the radius, and the displacement is a function of the radius only. There are only three nonzero stresses $(\sigma_r, \sigma_\theta, \sigma_\varphi)$ and strains $(\varepsilon_r, \varepsilon_\theta, \varepsilon_\varphi)$. By symmetry, we also have $\sigma_\theta = \sigma_\varphi$ and $\varepsilon_\theta = \varepsilon_\varphi$. Then the equilibrium equations reduce to

$$r\frac{d\sigma_r}{dr} + 2(\sigma_r - \sigma_\theta) = 0. \tag{9}$$

From elastic solution and yield function, the initial yield pressure is

$$P_c = \frac{2\sqrt{3}}{3(1-\alpha)}Y. \tag{10}$$

Equation (10) is plotted in Fig. 85.10. With the increase of α, the material yields at higher inner pressure.

It can be proved that $\sigma_\theta > \sigma_r$ at any point, so the effective stress can be simplified to

$$\sigma_e = -\frac{\alpha}{3}(\sigma_r + 2\sigma_\theta) + \frac{1-\alpha}{\sqrt{3}}(\sigma_\theta - \sigma_r). \tag{11}$$

With the help of the yield function, the relation of stresses in a plastic zone is solved by

$$\sigma_\theta = \frac{3Y + \left[\sqrt{3} - \alpha\left(\sqrt{3}-1\right)\right]}{\sqrt{3} - \alpha\left(2+\sqrt{3}\right)}\sigma_r\,. \tag{12}$$

Substituting Eq. (12) into the equilibrium Eq. (9), the stresses in the plastic zone are

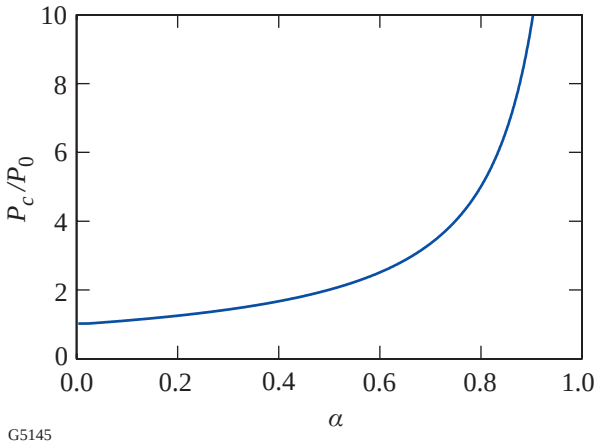

Figure 85.10
Initial yield pressure versus densification parameter. P_0 is the initial yield pressure without densification.

$$\sigma_r = -\frac{Y}{\alpha} + C r^{\frac{6\alpha}{\sqrt{3}-\left(2+\sqrt{3}\right)\alpha}},$$

$$\sigma_{\theta,\varphi} = -\frac{Y}{\alpha} + C\frac{\sqrt{3}-\left(\sqrt{3}-1\right)\alpha}{\sqrt{3}-\left(2+\sqrt{3}\right)\alpha} r^{\frac{6\alpha}{\sqrt{3}-\left(2+\sqrt{3}\right)\alpha}}, \tag{13}$$

where C can be solved from the boundary condition at the cavity wall ($r = a$). At the plastic–elastic boundary ($r = b$), traction continuity gives

$$\left(\frac{b}{a}\right)^{\frac{6\alpha}{\left(2+\sqrt{3}\right)\alpha-\sqrt{3}}} = \frac{\sqrt{3}(1-\alpha)\left(1-\alpha\frac{P}{Y}\right)}{\sqrt{3}-\left(2+\sqrt{3}\right)\alpha}. \tag{14}$$

It can be easily verified that $b \geq a$ if and only if $P > P_c$.

For the cavity problem, the flow potential [Eq. (4)] is

$$g = -\alpha'\frac{\sigma_r+\sigma_\theta+\sigma_\varphi}{3} + \frac{1-\alpha'}{2\sqrt{3}}\left(\sigma_\theta-\sigma_r\right) + \frac{1-\alpha'}{2\sqrt{3}}\left(\sigma_\varphi-\sigma_r\right). \tag{15}$$

By the flow theory $d\varepsilon_{ij}^p = d\lambda\partial g/\partial\sigma_{ij}$, we have

$$d\varepsilon_r^p = d\lambda\left(-\frac{\alpha'}{3}-\frac{1-\alpha'}{\sqrt{3}}\right),$$

$$d\varepsilon_\theta^p = d\lambda\left(-\frac{\alpha'}{3}+\frac{1-\alpha'}{2\sqrt{3}}\right), \tag{16}$$

$$d\varepsilon_\varphi^p = d\lambda\left(-\frac{\alpha'}{3}+\frac{1-\alpha'}{2\sqrt{3}}\right).$$

From the elastic theory, the elastic strain rate is

$$d\varepsilon_r^e = \frac{1}{E}\left(d\sigma_r - 2\nu d\sigma_\theta\right),$$

$$d\varepsilon_\theta^e = d\varepsilon_\varphi^e = \frac{1}{E}\left[-\nu d\sigma_r + (1-\nu)d\sigma_\theta\right]. \tag{17}$$

The total strain rate contains both elastic and plastic parts: $d\varepsilon_{ij} = d\varepsilon_{ij}^e + d\varepsilon_{ij}^p$. By eliminating the $d\lambda$, we have

$$A' d\varepsilon_r + 2d\varepsilon_\theta = \frac{1}{E}\left\{(A'-2\nu)d\sigma_r + 2\left[1-(1+A')\nu\right]d\sigma_\theta\right\},$$

$$A' = \frac{\sqrt{3}-\left(2+\sqrt{3}\right)\alpha'}{\sqrt{3}-\left(\sqrt{3}-1\right)\alpha'}. \tag{18}$$

Hill has solved this problem for the shear flow theory.[8] Following his method, the displacement increment can be written as

$$du(r,b) = \frac{\partial u}{\partial b}db + \frac{\partial u}{\partial r}dr = \left(\frac{\partial u}{\partial b} + v\frac{\partial u}{\partial r}\right)db, \tag{19}$$

where v is defined as the "velocity" of the particle. Defined in terms of the total displacement u and plastic–elastic boundary b,

$$v = \frac{\frac{\partial u}{\partial b}}{1-\frac{\partial u}{\partial r}}. \tag{20}$$

Written in terms of v and db, the nonzero stress and stain increments are

$$d\varepsilon_r = \frac{\partial}{\partial r}(du) = \frac{\partial v}{\partial r}db,$$

$$d\varepsilon_\theta = \frac{du}{r} = \frac{v db}{r},$$

$$d\sigma_r = \left(\frac{\partial\sigma_r}{\partial b} + v\frac{\partial\sigma_r}{\partial r}\right)db, \tag{21}$$

$$d\sigma_\theta = \left(\frac{\partial\sigma_\theta}{\partial b} + v\frac{\partial\sigma_\theta}{\partial r}\right)db.$$

Substituting Eqs. (21) and (13) into (18), we have

$$A'\frac{\partial v}{\partial r}+\frac{2v}{r}=\frac{Y}{E}\,\frac{2\sqrt{3}}{1-\alpha}\left(\frac{b}{r}\right)^{\frac{6\alpha}{(2+\sqrt{3})\alpha-\sqrt{3}}}\left(\frac{v}{r}-\frac{1}{b}\right)$$
$$\times\left[\left(A'+\frac{2}{A}\right)-\left(2+2\frac{A'}{A}+\frac{2}{A}\right)v\right], \quad (22)$$
$$A=\frac{\sqrt{3}-(2+\sqrt{3})\alpha}{\sqrt{3}-(\sqrt{3}-1)\alpha}.$$

This is a first-order partial differential equation for v. By integrating Eq. (22) from the cavity wall ($r=a$) to the plastic–elastic boundary ($r=b$), the problem is solved. Equation (22) is coupled (via a, b) and subject to numerical integration. The fourth-order Runge–Kutta method is used to solve this equation. For verification, the problem is also solved by using the finite-element package Abaqus (Hibbitt, Karlssoon, & Sorensen, Inc.). The large deformation theory is used in the finite-element simulation.

Associated Flow Theory

For the associated flow theory, $\alpha=\alpha'$ and $A=A'$. The flow potential coincides with the yield surface. Perfect plastic deformation is also assumed. Pressure–expansion curves are shown in Fig. 85.11 from both the finite-element and numerical integration results. It is interesting that with the increase of α the material becomes "softer" for small α and "harder" for large α. It is also noticed that for small α, there is a pressure limit for cavity expansion, as expected for perfect-plastic material deformed with shear flow only. When the inner pressure is close to this limit, the cavity expands spontaneously. For large α, we do not see this pressure limit. The difference between finite-element and numerical integration results is due to the use of the finite deformation theory in the finite-element simulation.

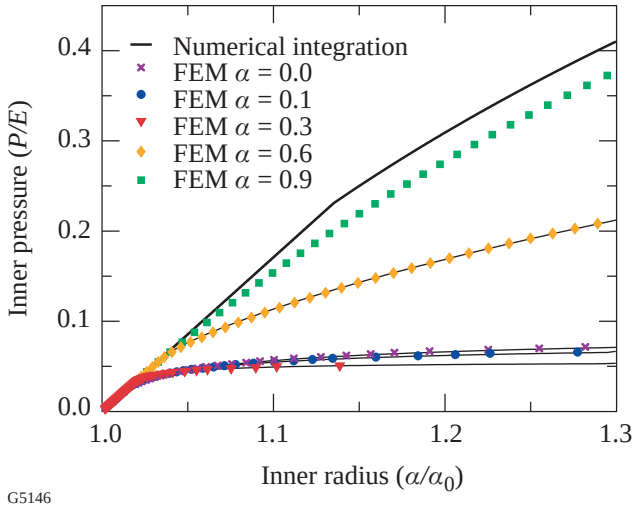

Figure 85.11
Cavity pressure–expansion curves for different α's.

The densification parameter α also affects the distribution of stresses at maximum load. The stresses at maximum load (1.45 P_c) are plotted in Figs. 85.12(a) and 85.12(b). For small α, the hoop stress is compressive; for large α, the hoop stress is tensile. We know that fracture under load is controlled by these stresses. For small α, if there is fracture under load, it happens under the surface; for large α, it will happen at the surface.

The residual stresses after 1.45 P_c loading are plotted in Figs. 85.12(c) and 85.12(d) for $\alpha=0.3$ and 0.6. The densification parameter also affects the residual stresses. For small α, the surface layer is under compression; for large α, it is under tension. The layer with large residual stresses is thicker for small α. It needs to be mentioned that the initial yield pressure P_c will increase with α, so we expect, under the same load, even smaller residual stresses for large α. It is observed that fused silica has smaller residual stresses after grinding.[9] Figure 85.12(e) also compares the hoop stress under the same load for $\alpha=0.1$, 0.3, and 0.6. At this load, only elastic deformation occurs for $\alpha=0.6$.

Non-associated Flow Theory

For the non-associated flow theory, the material behavior is controlled by both yield function [Eq. (1)] and plastic potential [Eq. (4)]; now α is not equal to α'. Thus we have three material parameters (α, α', Y) to describe the plastic deformation. The reasonable combinations of α and α' should be investigated. It is not possible to have $\alpha=1$ and $\alpha'=0$, which means that the material yields with pressure but can be permanently deformed only with shear.

The integration of Eq. (22) has been carried out numerically for different combinations of α and α'. The results for $\alpha=0.3$ and $\alpha=0.6$ are shown in Fig. 85.13. When $\alpha=0.3$, it is physically impossible for $\alpha'=0.6$ and 0.9, which means that the cavity cannot decrease in size with an increase in inner pressure. For the same reason, α' cannot be 0.1 or 0.3 for $\alpha=0.6$. From the analysis, we found the number separating these two regions to be around 0.46. These findings have been summarized in Fig. 85.14. For small α, α' must be small and vice versa.

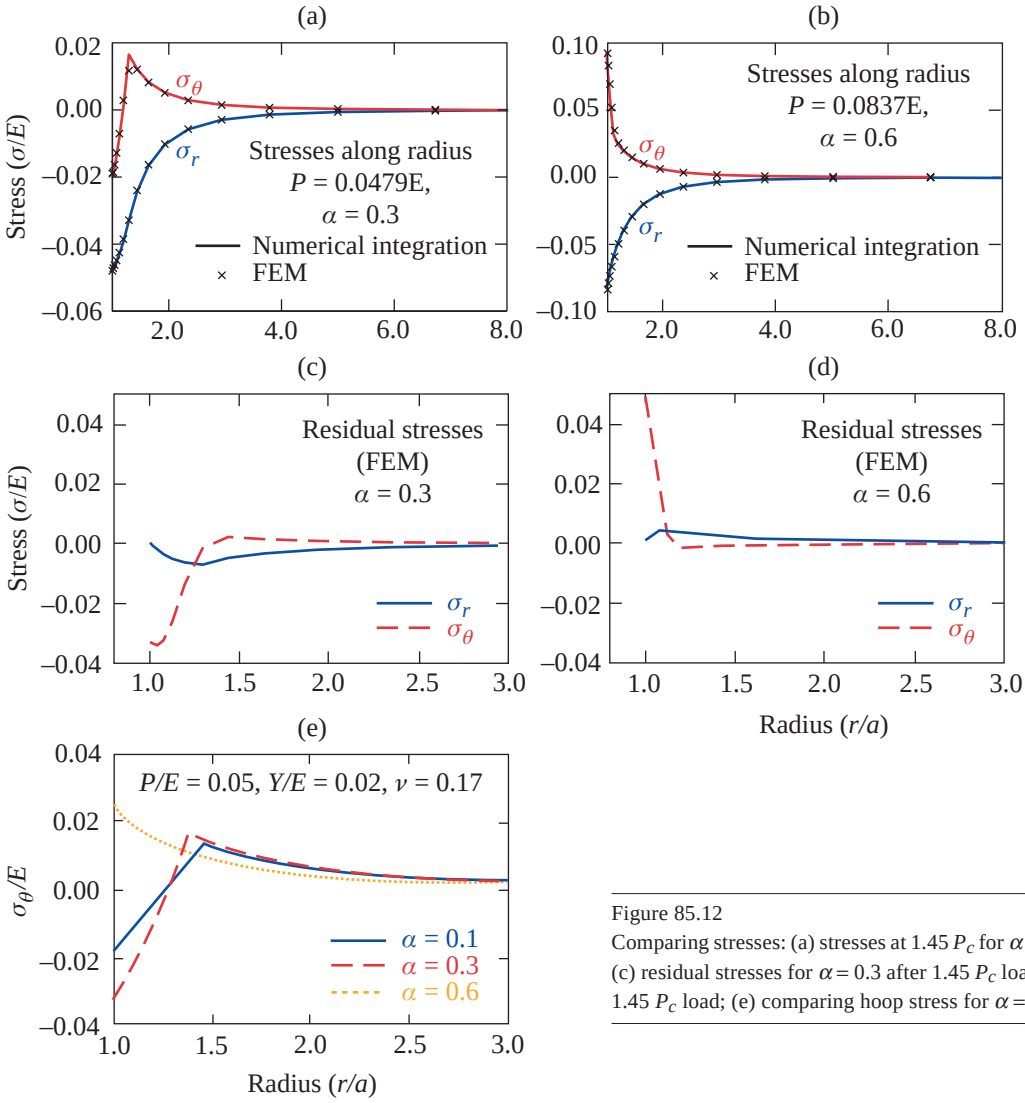

Figure 85.12
Comparing stresses: (a) stresses at 1.45 P_c for $\alpha = 0.3$; (b) stresses at 1.45 P_c for $\alpha = 0.6$; (c) residual stresses for $\alpha = 0.3$ after 1.45 P_c load; (d) residual stresses for $\alpha = 0.6$ after 1.45 P_c load; (e) comparing hoop stress for $\alpha = 0.1$, 0.3, and 0.6.

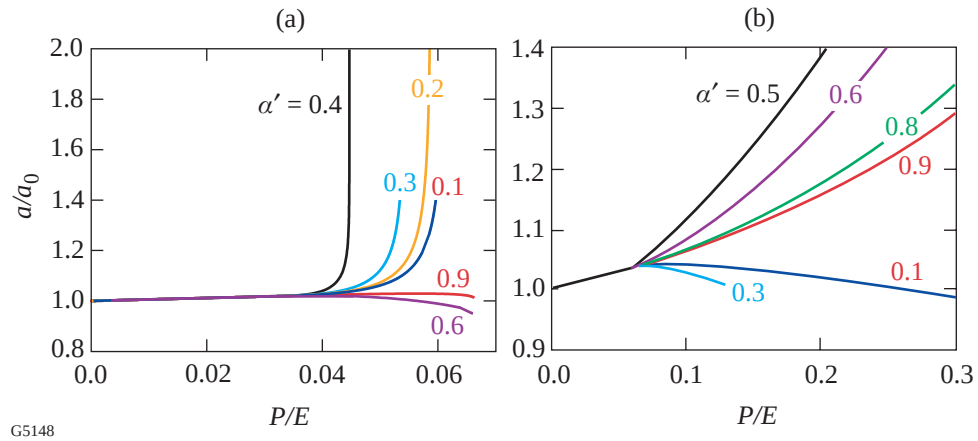

Figure 85.13
Pressure–expansion curves for non-associated flow theory: (a) $Y/E = 0.02$, $\alpha = 0.3$; (b) $Y/E = 0.02$, $\alpha = 0.6$.

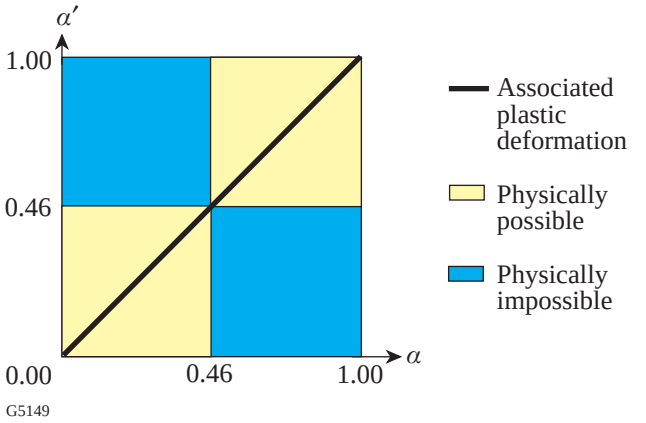

Figure 85.14
Material possibility map.

Figure 85.13(a) shows the pressure expansion curves for small α and α'. As observed in the associated theory, there is a pressure limit for spontaneous growth. For small α, with the increase of α', the limit pressure decreases, which means that the material becomes "softer." The spontaneous growth pressure is not observed for large α and α' [see Fig. 85.13(b)]. We also noticed that, for large α, the material becomes "harder" with the increase of α'.

Conclusion

The cavity problem has been studied by using a new material model. Both associated and non-associated flow theories have been examined. For the associated case, $\alpha = \alpha'$ and plastic potential is coincident with yield surface. We have two material parameters (α, Y) to describe plastic deformation with densification. The initial yield pressure increases with α. When α is small (small densification), there is a small softening with the increase of α. The cavity can grow spontaneously when the inner pressure reaches a limit. When α is large (large densification), there is a remarkable strengthening with the increase of α. The spontaneous cavity growth is not observed. The densification affects stress distributions at loading. When the densification parameter α is small, the hoop stress under load is compressive, similar to the material flowing without densification. When α is large, the hoop stress under load is tensile. The residual stresses are also affected by densification. For small densification, the surface residual stress is compressive; it is tensile for large densification.

For the non-associated case, the plastic behavior is described by three material parameters: α, α', Y. By investigating the non-associated case, we found that there are physically impossible combinations for α and α'. It is necessary to keep both α and α' small (<0.46) or large (>0.46). The increase of α' causes softening for small α and hardening for large α.

REFERENCES

1. P. W. Bridgman and I. Simon, J. Appl. Phys. **24**, 405 (1953).
2. R. Roy and H. M. Cohen, Nature **190**, 789 (1961).
3. E. B. Christiansen, S. S. Kistler, and W. B. Gogarty, J. Am. Ceram. Soc. **45**, 172 (1962).
4. J. D. Mackenzie, J. Am. Ceram. Soc. **46**, 461 (1963).
5. J. S. Tse, D. D. Klug, and Y. Le Page, Phys. Rev. B **46**, 5933 (1992).
6. J. C. Lambropoulos, S. Xu, and T. Fang, J. Am. Ceram. Soc. **79**, 1441 (1996).
7. A. B. Shorey, K. Xin, K.-H. Chen, and J. C. Lambropoulos, in *Inorganic Optical Materials*, edited by A. J. Marker III (SPIE, Bellingham, WA, 1998), Vol. 3424, pp. 72–81.
8. R. Hill, *The Mathematical Theory of Plasticity* (Clarendon Press, Oxford, 1950).
9. J. C. Lambropoulos, S. Xu, T. Fang, and D. Golini, Appl. Opt. **35**, 5704 (1996).